Supplementary Materials

Materials and Methods in detail

Supplementary Figure 1. Illustration of human tissues collection and determination of TNC expression in AS.

Supplementary Figure 2. TNC is up-regulated in DBA/1 model and CAIA model.

Supplementary Figure 3. Inhibition of TNC suppresses entheseal pathological new bone formation.

Supplementary Figure 4. The successful creation of the TNC KO mice.

Supplementary Figure 5. TNC is critical for chondrogenesis in the process of endochondral ossification.

Supplementary Figure 6. TNC-mediated reduction in matrix adhesion force activates Hippo/YAP signalling.

Supplementary Figure 7. TNC is majorly secreted by fibroblast-specific protein-1 (FSP1)+ fibroblasts.

Materials and Methods in detail

Patient and Public Involvement

Patients or the public were not involved in the design, or conduct, or reporting, or dissemination plans of our research.

Patients

With ethics committee approval and patient consent, the samples (bone, ligamentum flavum, supraspinatus ligament and interspinous ligament) involved in spinal ankylosis from AS patients and non-AS patients were collected during surgeries. Twenty-two patients (10 with AS and 12 with non-AS) were enrolled between September 2015 and June 2019. The indications of surgery for AS patients included disabling kyphosis, loss of horizontal vision without compensation, painful spinal pseudarthrosis or Andersson lesion.[1] Non-AS patients without any systemic inflammatory condition including SpA fulfilled the indications for correction of scoliosis or spinal decompression of thoracic or lumbar stenosis.[2-4]

Mice

DBA/1 and C57BL/6J mice were purchased from the Charles River Laboratories. The TNC knockout mouse model (C57BL/6J) was created by Cyagen Biosciences via using CRISPR/Cas-mediated genome engineering. Exon 3-5 of TNC gene (NCBI Reference Sequence: NM_011607.3; Ensembl: ENSMUSG00000028364) were selected as target site.

For spontaneous arthritis model, male DBA/1 mice (8 weeks) were mixed and caged together in groups of 9 mice to induce arthritis. For antibody administration, the mice received treatment intraperitoneally once a week with TNC-neutralizing antibody (5mg/kg) (MAB2138, R&D Systems) or the equivalent volume of vehicle antibody (MAB006, R&D Systems) since the

second week after caging. For Hippo pathway signaling inhibition, the mice received treatment intraperitoneally three times a week with XMU-MP-1 (2mg/kg) (HY-100526, a reversible and selective MST1/2 inhibitor, MedChemExpress) since the second week after caging. DMSO was administered as a negative control.

For CAIA model, WT and TNC knockout C57BL/6J mice (male, 10 weeks) were injected intraperitoneally with Arthrogen-CIA monoclonal antibody cocktail (4mg/20g) (Chondrex, Inc) on day 0. Then 100μg lipopolysaccharide (LPS) was injected intraperitoneally into each mouse on day 3. The equivalent volume of non-specific immunoglobulin (day 0) and LPS (day 3) were used for control purposes.

At the end of each experimental time point, mice were sacrificed. Hind paw specimens were dissected and fixed with 4% paraformaldehyde for μCT and histological analyses.

Human tissues collection

A typical image of CT scanning of an AS patient with different stages of the pathological process of new bone formation is showed in supplementary figure S1A. Position 1 (red) represents an early stage with no ossification, with clearly recognizable margin of the spinous process (SP) and the interspinous ligament. Position 2 (blue) represents an intermitted stage with partial ossification. Ossification of ligament is evident and the margins of the spinous process and the interspinous ligament is indistinct. Position 3 (green) represents an end stage of ossification with complete bony fusion. The spinous process and the interspinous ligament are completely fused together. In the current study, human spinal tissues were obtained at position 2 (red asterisk), which would potentially develope into pathological new bone.

Cell Culture

MSCs were isolated and purified by using density gradient centrifugation as previously described.[5] The samples were minced and digested with 1 mg/ml collagenase D (Roche). The digested specimens were filtered through a 40-μm nylon filter after overnight incubation at 37°C. After isolated and purified, MSCs were suspended in low-glucose DMEM (Gibco) supplemented with 10% FBS (Gibco) and 1% penicillin/streptomycin and cultured in humidified incubator at 37°C and 5% CO2.

RNA Sequencing and single cell RNA Sequencing

Samples collected from surgeries immediately enter the RNA extraction program. Total RNA was extracted using Trizol reagent kit (Invitrogen) according to the manufacturer's protocol. The total RNA of the samples was tested for integrity using agarose gel electrophoresis, and NanoDrop ND-1000 was used for quantification and further quality inspection. 1 ~ 2μg of total RNA per sample was selected for sequencing library construction. Total RNA was first enriched using the NEB Next® Poly (A) mRNA Magnetic Isolation Module. The processed RNA product was used for library construction through KAPA Stranded RNA-Seq Library Prep Kit (Illumina). The constructed library was tested by Agilent 2100 Bioanalyzer, and the library was finally quantified by qPCR. According to the quantitative results and the amount of final sequencing data, sequencing libraries that mix different samples were required to enter the sequencing process. Sequencing libraries of different mixed samples were denatured with 0.1M NaOH to generate single-stranded DNA, diluted to 8 pM, and amplified in situ on TruSeq SR Cluster Kit v3-cBot-HS (# GD-401-3001, Illumina) The end of the generated fragment was sequenced for 150 cycles using a sequencer such as Illumina HiSeq 4000.

Data was mapped to reference genome by TopHat2 (version 2.1.1), then transcripts abundances were quantified by software RSEM (version 1.2.19). Firstly, a set of reference

transcript sequences were generated and preprocessed according to transcripts (in FASTA format) and gene annotation files (in GTF format). Secondly, reads were realigned to the reference transcripts by Bowtie alignment program and the resulting alignments were used to estimate transcript abundances. The transcript expression level was normalized by using FPKM (Fragments Per Kilobase of transcript per Million mapped reads). Value of transcripts from the same gene were merged to obtain reads counts and expression level at gene level. Differentially expressed genes (DEGs) were also identified by the edgeR package (version 3.12.1) (http://www.r-project.org/) with general linear model and a threshold of fold change > 2 and FDR < 0.05.

For sc-RNA-seq, R1 (read 1 primer sequence) are added to the molecules during GEM incubation. P5, P7, a sample index, and R2 (read 2 primer sequence) are added during library construction via End Repair, A-tailing, Adaptor Ligation, and PCR. The final libraries contain the P5 and P7 primers used in Illumina bridge amplification. The Single Cell 3' Protocol produces Illumina-ready sequencing libraries. A Single Cell 3' Library comprises standard Illumina paired-end constructs which begin and end with P5 and P7. The Single Cell 3' 16 bp 10x Barcode and 10 bp UMI are encoded in Read 1, while Read 2 is used to sequence the cDNA fragment. Sample index sequences are incorporated as the i7 index read. Read 1 and Read 2 are standard Illumina® sequencing primer sites used in paired-end sequencing.

μCT analysis

All samples including ankles with feet and Achilles tendons were obtained from mice post-mortem and fixed with 4% paraformaldehyde. For μCT scanning, specimens were fitted in a cylindrical sample holder and scanned using a Scanco μCT40 scanner set to 55 kVp and 70 μA.

For visualization, the segmented data were imported and reconstructed as three-dimensional images using MicroCT Ray V3.0 software (Scanco Medical).

Histologic analyses

For histologic analysis, specimens were decalcified in 0.5M EDTA (Sigma-Aldrich) at 4°C. Paraffin-embedded or OCT compound-embedded tissues were sectioned at 4 μm intervals using a paraffin microtome (RM2235, LECIA) or a frozen slicer (HM550VP, MICROM). The sections being compared were taken at the same anatomical level to ensure that the following experiments were conducted on serial sections and stained. For haematoxylin and eosin (H&E), Toluidine Blue (TB) and Safranin O Fast Green (SOGF) staining, paraffin-embedded sections slides were dewaxed in xylene and stained by following the manufacturer's protocol to evaluate general structures and bone formation. Immunohistochemistry and immunofluorescence analysis were performed as described previously.[6] Both dewaxed paraffin sections and frozen sections were heated to 99°C for 20 minutes in citrate buffer (10 mM, pH 6.0) for antigen retrieval, and rehydrated. After washing three times with PBS, the tissue sections were incubated with primary antibodies to human TNC (Abcam, ab3970), Sox9 (Abcam, ab185230), mouse TNC (Abcam, ab108930), Collagen II (Abcam, ab185430), Aggrecan (Abcam, ab3778), Col X (Abcam, ab58632), Sca-1 (R&D, AF1226), YAP (CST, 14074S), Phospho-YAP (S127) (CST, 13008S), Sox9 (Novus Biologicals, CL0639), Actin (Abcam ab14128), FSP1 (Abcam, ab197896), CD45 (Abcam, ab40763), MMP13 (Abcam, ab39012), OCN (Abcam, ab13418) overnight at 4°C. For immunohistochemical staining, after blocking endogenous peroxidase with hydrogen peroxide solution, a horseradish peroxidase-diaminobenzidine detection kit (DA1010, SOLARBIO) was used. For immunofluorescence staining, after washing three times with PBS, tissue sections were incubated with the secondary antibody conjugated with Dylight-594 or Dylight-488 or Dylight-

649 fluorescence for 1 h at room temperature avoiding light before being imaged with confocal microscope (DM6B, LECIA). Images were processed using Leica Application Suite X software, and quantifications were performed using ImageJ software. Tissue sections were quantitated according to the number of positive cells in per area as previously described.[6]

Chondrogenic differentiation

In vitro chondrogenesis was performed using micromass culture by seeding 4×10^5 cells in 20 μl droplets. Chondrogenic differentiation of human mesenchymal stem cells was induced by treatment with 10 ng/ml of TGF-β1 (Gibco) in a chemically defined serum-free medium 24h after seeding and then stained with alcian blue at pH 1.0 after 7 days. Chondrogenic differentiation of ADTC5 cells was induced by treatment with BMP-2 (R&D) at 300ng/ml in DMEM (4.5 g/l glucose) in the presence of 10% FBS and 50 μg/ml ascorbic acid 3h after seeding and then stained with alcian blue at pH 1.0 after 7 days. For in vivo chondrogenesis, micromass-cultured MSCs were induced with chondrogenic medium for 3 d. The MSCs were then wrapped in the Transwell membrane and implanted subcutaneously into Nu/Nu mice. The specimens were dissected from recipient mice and analyzed 4 weeks later.[7]

Coating with purified ECM molecules

TNC (R&D, 3358-TC-050) and RGD peptides (GCGYGRGDSPG, Genscript) were coated on glass coverslips or Matrigel using protocols as previously described. Briefly, FN and TNC were coated in 0.01% Tween 20-PBS at 1-2 $\mu g/cm^2$ before saturation with 10 mg/ml heat inactivated BSA/PBS.[8, 9]

Quantitative real-time PCR

Total RNA was extracted using Trizol reagent (Invitrogen) according to the manufacturer's protocol. 2 μg of total DNA-free RNA was used to synthesize cDNA by using PrimeScript™ RT reagent Kit (Takara). Amplification reactions were set up in 96-well plates using iTaq™ SYBR Green Super mix (BIO-RAD), to which gene-specific forward and reverse PCR primers were added. These analyses were performed to detect TNC (sense, 5'-CCTTGCTGTAGAGGTCGTCA-3'; antisense, 5'-CCAACCTCAGACACGGCTA-3'), Sox9 (sense, 5'-AGGAAGCTGGCAGACCAGTA-3'; antisense, 5'-CGTTCTTCACCGACTTCCTC-3'), Aggrecan (sense, 5'-GTGGTGGAGCATGCTAGAACCC-3'; antisense, 5'-ATTCGAGGCTCTTCCCAGTGCC-3'), Col II (sense, 5'-ACTGGTAAGTGGGGCAAGAC-3'; antisense, 5'- CCACACCAAATTCCTGTTCA-3') expression, and GAPDH (sense, 5'-TGGCAAAGTGGAGATTGTTGC-3'; antisense, 5'-AAGATGGTGATGGGCTTCCCG-3') was used as an internal control.

Western blot

A 10% SDS-PAGE gel was loaded with 20 μg of total protein, and the separated proteins were transferred by electro blotting to PVDF membranes. The membranes were blocked with 5% non-fat dry milk in TBST and incubated with the primary antibody including anti-TNC antibody (Abcam, ab3970), anti-Sox9 antibody (Abcam, ab185230), anti-Aggrecan antibody (Abcam, ab3778), anti-Collagen II antibody (Abcam, ab185430), anti-Phospho-YAP (S127) antibody (CST, 13008S), anti-YAP (CST, 14074S), anti-Phospho-LATS1 (Ser909) (CST, 9157S), anti-LATS1 (CST, 3477S), anti-Rho (Sigma-Aldrich, 17-294), anti-GAPDH (CST, 5174S) and anti-β-tubulin antibody (Abcam, ab179513) overnight at 4°C. Immunolabelling was detected using ECL reagent (Thermo Fisher Scientific).

Atomic force microscopy measurements

Atomic force microscopy (AFM) measurement and analysis were performed using an Atomic Force Microscope (SPM-9500J3, Shimadzu Corporation, Japan) located at Chemistry and Chemical Engineering College, Sun Yat-sen University as previously described.[10-14] Briefly, freshly dissected tissues were OCT-embedded, flash-frozen in liquid nitrogen and sectioned at 20 μm intervals. After rinsing off optimal cutting temperature compound (OCT) using room temperature PBS, slides were then magnet-anchored to the stage of the microscope. All samples were measured in liquid media in contact mode using Novascan cantilevers (2.5-μm radius beaded silica glass tip, Spring Constant=0.05 N/m, Deflection Sensitivity= 80.58 nm/V), which were calibrated using the thermal tune method. Force measurements were collected over a 80 × 80μm grid. The resulting force data were converted to elastic modulus values using the Hertz Model program (tissue samples were assumed to be noncompressible, and a Poisson's ratio of 0.5 was used in the calculation of the Young's elastic modulus values). Data was processed using NanoScope Analysis software (Bruker Corporation).

Lentivirus Infection

Recombinant lentiviruses expressing YAP1 (5SA) were obtained from Genechem (Genechem, Shanghai, China). Recombinant lentiviruses targeting YAP1 (shYAP1, CCGGCGGTTGAAACAACAGGAATTACTCGAGTAATTCCTGTTGTTTCAACCGTTTTTG) and the scramble control (shNC) were predesigned by the online software (Sigma-Aldrich) and constructed by Gene Pharma (Gene Pharma, Suzhou, China). ADTC5 cells were incubated with lentivirus supernatant for 24 h and then transferred to growth medium containing G418 to select for stable transfectants.

Statistical analysis

Statistical analyses were performed using SPSS 22.0. All data obtained from experiments repeated at least three times was represented as mean ± SD. Differences between 2 groups were analyzed using 2-tailed Student's t test. Comparisons of multiple groups was analysed via one-way analysis of variance (ANOVA). The level of significance was set at $P<0.05$.

References:

1. Zochling J, van der Heijde D, Burgos-Vargas R et al. ASAS/EULAR recommendations for the management of ankylosing spondylitis. Ann Rheum Dis 2006;65: 442-52.
2. Lenke LG, Betz RR, Harms J et al. Adolescent idiopathic scoliosis: a new classification to determine extent of spinal arthrodesis. J Bone Joint Surg Am 2001;83: 1169-81.
3. Kreiner DS, Shaffer WO, Baisden JL et al. An evidence-based clinical guideline for the diagnosis and treatment of degenerative lumbar spinal stenosis (update). Spine J 2013;13: 734-43.
4. Watters WC, Bono CM, Gilbert TJ et al. An evidence-based clinical guideline for the diagnosis and treatment of degenerative lumbar spondylolisthesis. Spine J 2009;9: 609-14.
5. Liu CH, Raj S, Chen CH et al. HLA-B27-mediated activation of TNAP phosphatase promotes pathogenic syndesmophyte formation in ankylosing spondylitis. J Clin Invest 2019;129: 5357-5373.
6. Li X, Chen S, Hu Z et al. Aberrant upregulation of CaSR promotes pathological new bone formation in ankylosing spondylitis. EMBO Mol Med 2020;12: e12109.
7. Tang Y, Rowe RG, Botvinick EL et al. MT1-MMP-dependent control of skeletal stem cell commitment via a β1-integrin/YAP/TAZ signaling axis. Dev Cell 2013;25: 402-16.
8. Sun Z, Schwenzer A, Rupp T et al. Tenascin-C Promotes Tumor Cell Migration and Metastasis through Integrin α9β1-Mediated YAP Inhibition. Cancer Res 2018;78: 950-961.

9. Kim IL, Khetan S, Baker BM et al. Fibrous hyaluronic acid hydrogels that direct MSC chondrogenesis through mechanical and adhesive cues. Biomaterials 2013;34: 5571-80.
10. Miroshnikova YA, Mouw JK, Barnes JM et al. Tissue mechanics promote IDH1-dependent HIF1α-tenascin C feedback to regulate glioblastoma aggression. Nat Cell Biol 2016;18: 1336-1345.
11. Trache A, Xie L, Huang H et al. Applications of Atomic Force Microscopy for Adhesion Force Measurements in Mechanotransduction. Methods Mol Biol 2018;1814: 515-528.
12. Li Z, Liu T, Yang J et al. Characterization of adhesion properties of the cardiomyocyte integrins and extracellular matrix proteins using atomic force microscopy. J Mol Recognit 2020;33: e2823.
13. Dao L, Gonnermann C, Franz CM. Investigating differential cell-matrix adhesion by directly comparative single-cell force spectroscopy. J Mol Recognit 2013;26: 578-89.
14. Friedrichs J, Werner C, Müller DJ. Quantifying cellular adhesion to covalently immobilized extracellular matrix proteins by single-cell force spectroscopy. Methods Mol Biol 2013;1046: 19-37.

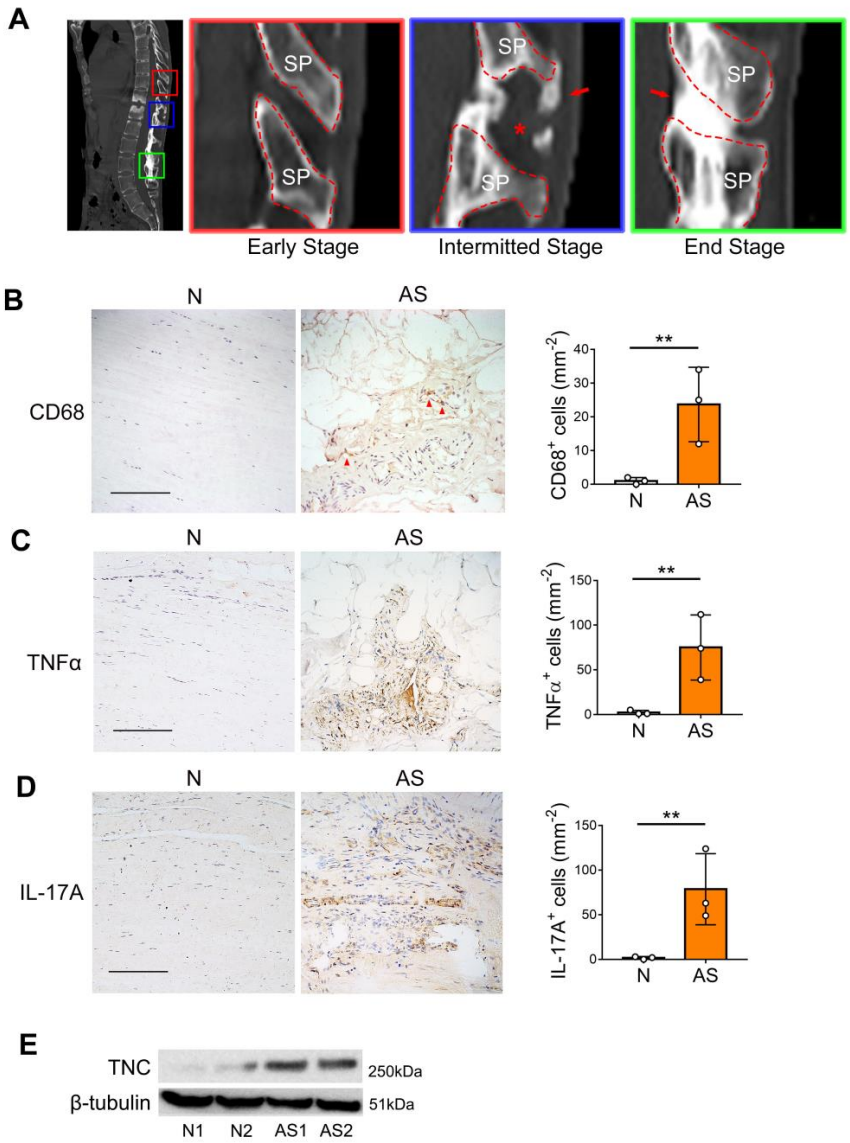

Supplementary Figure 1. Illustration of human tissues collection and determination of TNC expression in AS

(A) CT scanning image showing early (red), intermitted (blue) and end stage (green) of the pathological process of new bone formation. Red arrows indicate pathological new bone; Red asterisk indicates uncalcified ligament; SP: spinous process. **(B)** Immunohistochemistry staining and quantitative analysis of CD68 in human spinal tissues. n=3. **(C)** Immunohistochemistry staining and quantitative analysis of TNFα in human spinal tissues. n=3. **(D)** Immunohistochemistry staining and quantitative analysis of IL-17A in human spinal tissues. n=3. **(E)** Western blot analysis of TNC expression in the human spinal tissue samples. Each group included 3 tissue samples collected from AS patients or non-AS controls. N, non-AS. Scale bar: 200μm. Data are presented as mean ± s.d. ** $p<0.01$. unpaired t-test in (B-D).

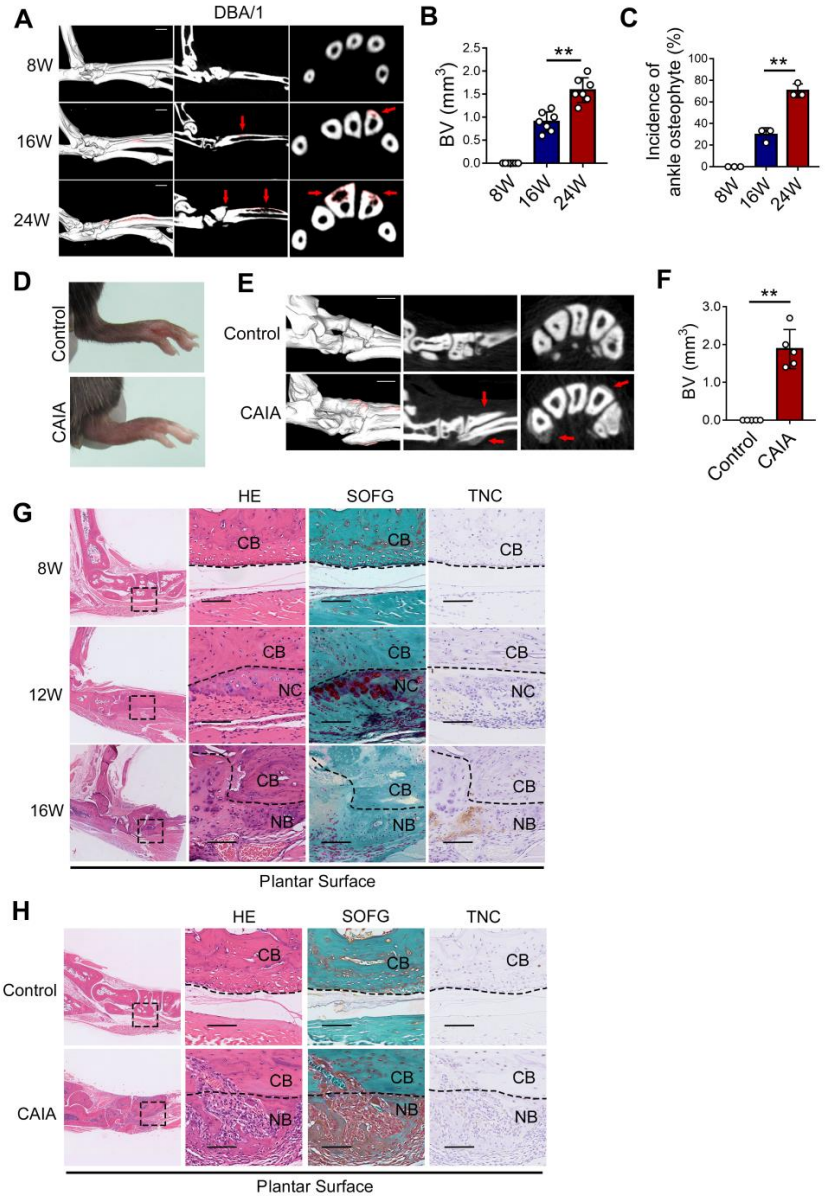

Supplementary Figure 2. TNC is up-regulated in DBA/1 model and CAIA model

(A-B) μCT images and quantitative analysis of new bone formation in male DBA/1 model. Red arrows indicate the new bone. n=7 per group. Scale bar: 1mm. **(C)** Incidence of new bone formation in male DBA/1 model. n=9 per cage of total 3 cages. **(D)** Representative images of hind paws of control mice and collagen antibody induced arthritis (CAIA) mice. **(E-F)** μCT images and quantitative analysis of hind paws of control mice and CAIA mice. Red arrows indicate the new bone. n=5 per group. Scale bar: 1mm. **(G)** H&E staining, SOFG staining and immunohistochemical analysis of TNC in plantar surface of hind paws of male DBA/1 mice. CB: cortical bone; NC: new cartilage; NB: new bone. Scale bar: 100μm. **(H)** H&E staining, SOFG staining and immunohistochemical analysis of TNC in hind paws of control mice and CAIA mice. Scale bar: 100μm. Data are presented as mean ± s.d. ** p<0.01. paired t-test in (B-C). unpaired t-test in (F).

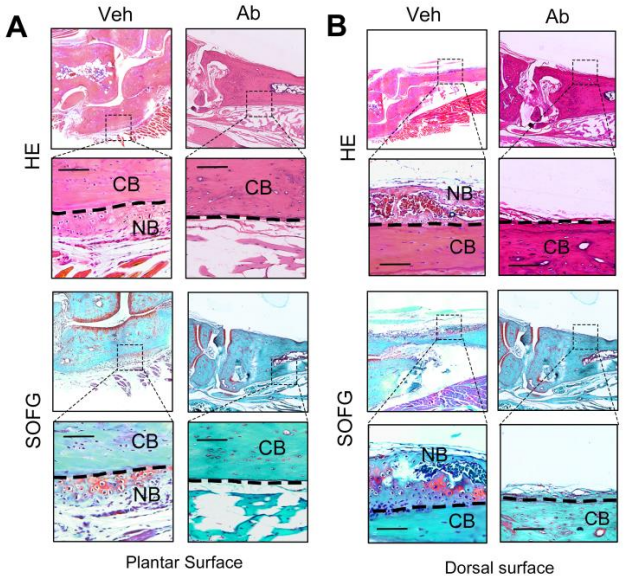

Supplementary Figure 3. Inhibition of TNC suppresses entheseal pathological new bone formation

(A-B) H&E staining and SOFG staining in plantar surface and dorsal surface of hind paws of male DBA/1 mice at the age of 16w. Veh: vehicle; Ab: antibody; CB: cortical bone; NB: new bone. Scale bar: 100μm.

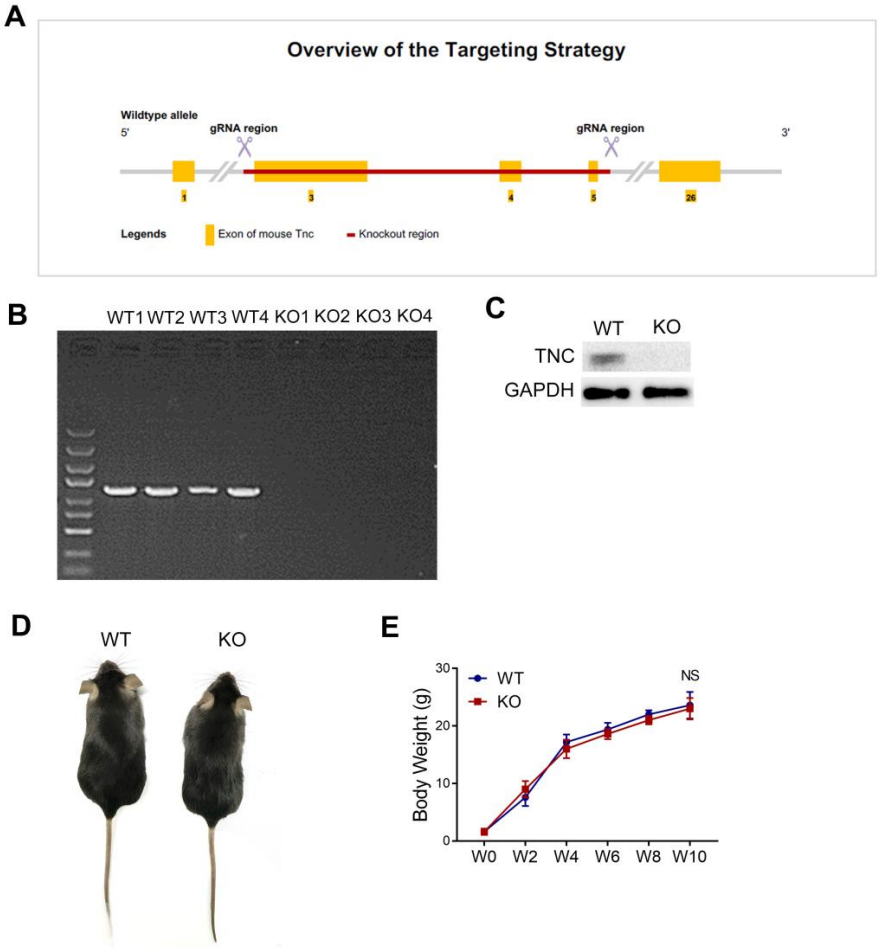

Supplementary Figure 4. The successful creation of the TNC KO mice

(A) Schematic diagram illustrating the targeting strategy. **(B)** Gel electrophoresis results of the PCR amplifications of RNA from cerebellum of WT mice and KO mice. **(C)** Western blot analysis of TNC from pooled extracts of cerebellum, lung, and thymus in WT mice and KO mice. **(D)** The appearance and **(E)** body weight of wild type mice and knockout mice. Data are presented as mean ± s.d. WT, wild type. KO, knockout.

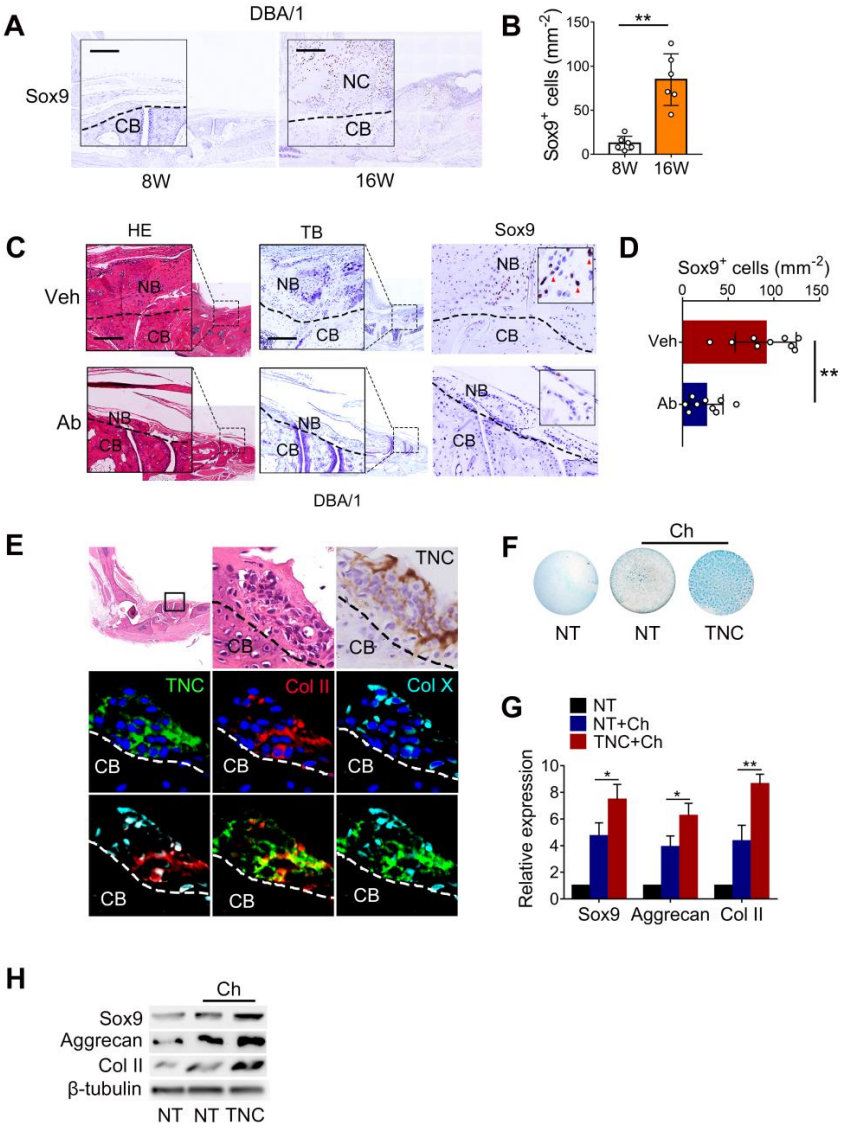

Supplementary Figure 5. TNC is critical for chondrogenesis in the process of endochondral ossification

(A) Immunohistochemical results of Sox9 in hind paws of male DBA/1 mice. CB: cortical bone; NC: new cartilage. Scale bar: 200μm. **(B)** Quantitative analysis of Sox9-positive cells (mm^{-2}) in immunohistochemical staining. n=6 per group. **(C)** H&E staining, toluidine blue staining and immunohistochemical analysis of Sox9 in hind paws of male DBA/1 model. NB: new bone. Scale bar: 200μm. **(D)** Quantitative analysis of Sox9-positive cells. n=9 per group. **(E)** H&E staining, immunohistochemical staining of TNC and immunofluorescence staining in male DBA/1 mice. CB: cortical bone. **(F)** Alcian blue staining of human mesenchymal stem cells planted on TNC-coated culture dish in micromass cultures for 7 days. Ch: chondrogenic medium. **(G-H)** Western blot analysis and qRT-PCR analysis of the level of Sox9, Aggrecan, Collagen II in human mesenchymal stem cells planted on TNC-coated culture dish in micromass cultures for 48h. Data are presented as mean ± s.d. * $p<0.05$. ** $p<0.01$. unpaired t-test.

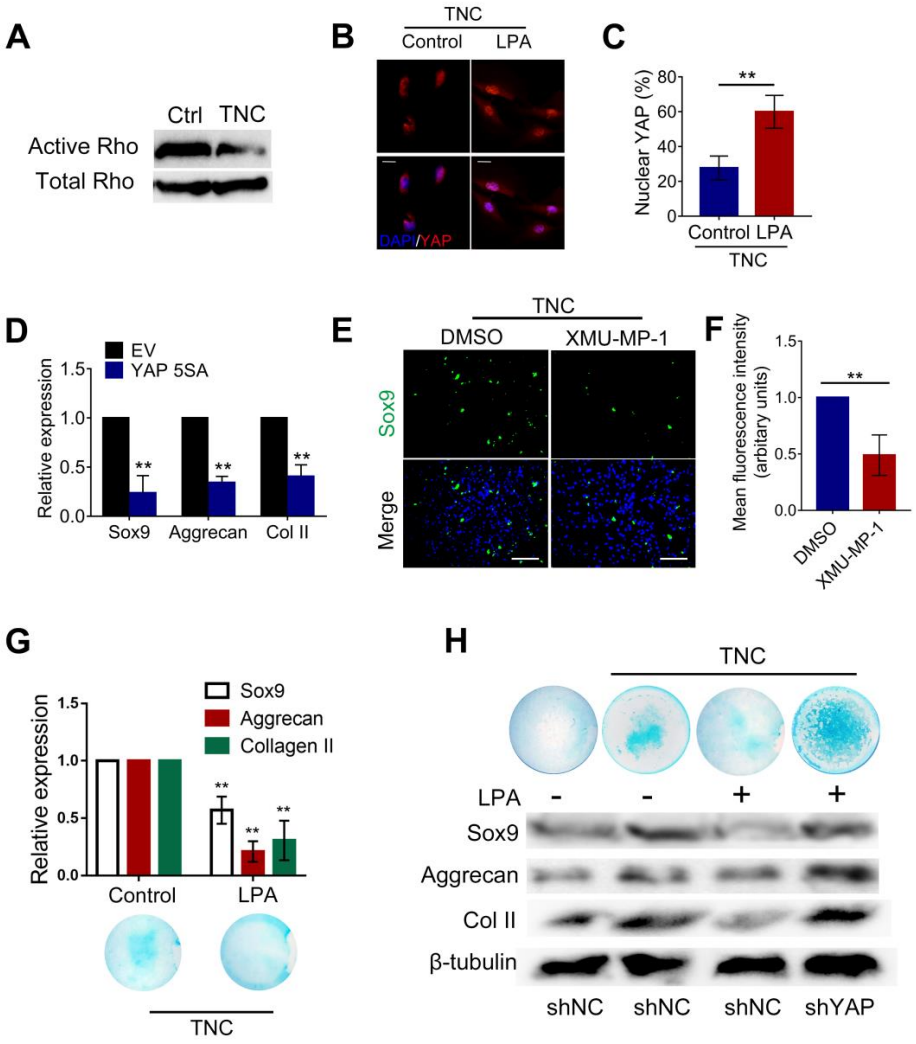

Supplementary Figure 6. TNC-mediated reduction in matrix adhesion force activates Hippo/YAP signalling

(A) Western blot analysis of the active and total Rho GTPase protein levels in ADTC5 cells plated on TNC for 24h. Ctrl: fibronectin 1. **(B)** Representative immunofluorescence image of YAP (Red) and nuclei (DAPI, Blue) in ADTC5 cells plated on TNC with or without administration of LPA for 12h. Scale bar: 10μm. **(C)** Percentage of nuclear YAP in (B). n=5. **(D)** qRT-PCR analysis of the levels of Sox9, Aggrecan and Collagen II in ADTC5 cells cultured on TNC transfected with Empty vector or YAP-overexpressing vector for 48h. **(E)** Immunofluorescence image of Sox9 (Green) in ADTC5 cells plated on TNC with application of XMU-MP-1 or DMSO for 48h. Scale bar: 100μm. **(F)** Mean fluorescence intensity of Sox9 in arbitrary units of (E). n=3. **(G)** qRT-PCR analysis and Alcian blue staining of ADTC5 cells plated on TNC with or without administration of LPA. **(H)** Alcian blue staining and western blot analysis of Sox9, Aggrecan and Collagen II in ADTC5 cells with or without administration of LPA and transfection of YAP shRNA. Data are presented as mean ± s.d. ** $p<0.01$. unpaired t-test.

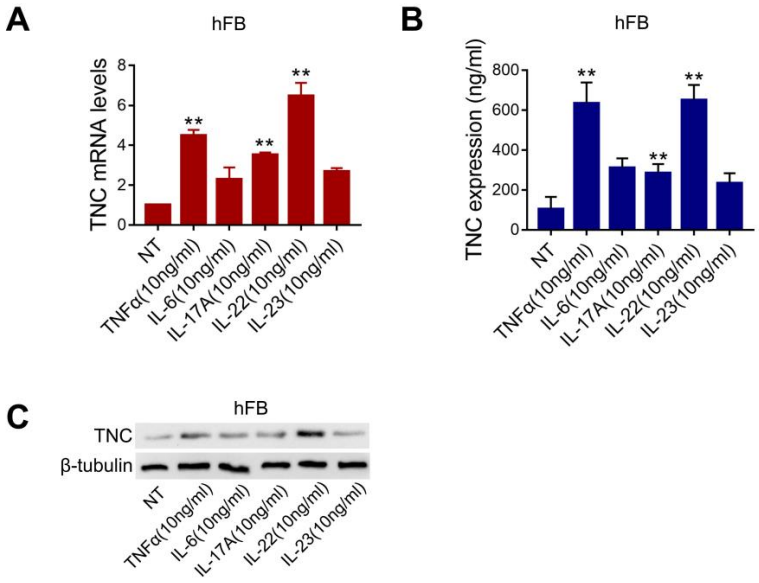

Supplementary Figure 7. TNC is majorly secreted by fibroblast-specific protein-1 (FSP1)+ fibroblasts

(A) qRT-PCR analysis of the levels of TNC in human fibroblasts (hFB) treated with TNFα, IL-6, IL-17A, IL-22 and IL-23. **(B)** ELISA analysis of TNC expression in human fibroblasts treated with TNFα, IL-6, IL-17A, IL-22 and IL-23. **(C)** Western Bolt analysis of TNC protein levels in human fibroblasts treated with TNFα, IL-6, IL-17A, IL-22 and IL-23. N, non-AS. Data are presented as mean ± s.d. ** $p<0.01$. unpaired t-test.